

above a threshold), the depleted fraction was very sensitive to source conditions, such as the time difference between the opening of the pulsed valve and the impact of the laser on the graphite rod (see Fig. 5), the duration of the gas pulse, or the location of the laser impact on the rod. Under some conditions, the depleted fraction was reduced to ~10%. Very little depletion variation was observed at the two other photon energies. In comparison with the Cs sputter source results, some reduction of the depleted fraction was observed. These results are consistent with cooling of the C_4^- clusters in the pulsed nozzle source because the region just above the measured threshold is very sensitive to the thermal vibrational state population of the negative cluster. The variation between the Cs sputter and the laser vaporization source indicates that the method of production of the clusters changes the ratio between the different isomers present in the beam.

Why were the lower thresholds found in the present experiment not detected in the previous experiments? Two possibilities can be advanced. First, as described above, the method of formation influences the population ratio between the different isomers. Thus, it is possible that some types of ion sources would preferentially "quench" the low-affinity population. In previous experiments, slightly different ion sources were used [supersonic expansion with "waiting room" (6) and high-energy vaporization laser]. Another possibility is the difference in the photodetachment sensitivity of the experimental methods. Previous experiments measured the threshold with electron spectroscopy with a higher laser energy (4.66 or 3.5 eV). The main electron signal comes from the transition having the largest cross section, thus overlooking the lower transition. An example of this phenomenon can be seen in the recent study by Arnold *et al.* (6), where for C_3 , the transition to the $^3\Pi_u$ excited state is much stronger than the transition to the $^1\Sigma_g^+$ ground state. In the same paper, high electron kinetic energy tails are found for some of the clusters at the lowest photon energy used (3.5 eV).

REFERENCES AND NOTES

1. W. Weltner, Jr., and R. J. van Zee, *Chem. Rev.* **89**, 1713 (1989).
2. K. S. Pitzer and E. Clementi, *J. Am. Chem. Soc.* **81**, 4477 (1959).
3. K. Raghavachari, R. A. Whiteside, J. A. Pople, *J. Chem. Phys.* **85**, 6623 (1986); R. J. van Zee, R. F. Ferrante, K. J. Zeringue, W. Weltner Jr., *ibid.* **86**, 5212 (1987); D. E. Bernholdt, D. H. Magers, R. J. Bartlett, *ibid.* **89**, 3612 (1988), and references therein.
4. S. Yang *et al.*, *Chem. Phys. Lett.* **144**, 431 (1988).
5. C. A. Schmuttenmaer *et al.*, *Science* **249**, 897 (1990); J. R. Heath, A. L. Cooksy, M. H. W. Gruebele, C. A. Schmuttenmaer, R. J. Saykally, *ibid.* **244**, 564 (1989); J. R. Heath, R. A. Sheeks,

- A. L. Cooksy, R. J. Saykally, *ibid.* **249**, 895 (1990); J. R. Heath and R. J. Saykally, *J. Chem. Phys.* **94**, 1724 (1991); H. Sasada, T. Amano, C. Jarman, P. F. Bernath, *ibid.*, p. 2401; N. Moazzen-Ahmadi, A. R. W. McKellar, T. Amano, *ibid.* **91**, 2140 (1989); *Chem. Phys. Lett.* **157**, 1 (1989).
6. D. W. Arnold, S. E. Bradforth, T. N. Kitsopoulos, D. M. Neumark, *J. Chem. Phys.* **95**, 8753 (1991).
7. G. von Helden, M.-T. Hsu, P. R. Kemper, M. T. Bowers, *ibid.*, p. 3835.
8. M. Algranati *et al.*, *J. Phys. Chem.* **90**, 4617

- (1989).
9. _____, *Isr. J. Chem.* **30**, 79 (1990).
10. Z. Vager, R. Naaman, E. P. Kanter, *Science* **244**, 426 (1989).
11. We thank M. Algranati and N. Altstein for their dedicated efforts. Supported in part by the U.S.-Israel Binational Science Foundation, the MIN-ERVA Fund, Munich, Germany, and the Basic Research Foundation administered by the Israel Academy of Science and Humanities.

15 June 1992; accepted 15 September 1992

A Liquid-Solution-Phase Synthesis of Crystalline Silicon

James R. Heath

A liquid-solution-phase technique for preparing submicrometer-sized silicon single crystals is presented. The synthesis is based on the reduction of $SiCl_4$ and $RSiCl_3$ ($R = H, \text{ octyl}$) by sodium metal in a nonpolar organic solvent at high temperatures (385°C) and high pressures (>100 atmospheres). For $R = H$, the synthesis produces hexagonal-shaped silicon single crystals ranging from 5 to 3000 nanometers in size. For $R = \text{octyl}$, the synthesis also produces hexagonal-shaped silicon single crystals; however, the size range is controlled to 5.5 ± 2.5 nanometers.

Crystalline Si is one of the most useful and exploited materials in modern technology. Indeed, single-crystal Si wafers form the foundation of the electronics industry. Polycrystalline Si finds applications in the fabrication of microcircuitry and photocells. Because of its many applications, much research and development have been aimed at producing high-quality crystalline and polycrystalline Si (1). Well-established methods for the production of single-crystal thin films include molecular beam epitaxy of evaporated Si and chemical vapor deposition of silanes, polysilanes, and halosilanes. Methods for the production of large single crystals include the Czochralski (2) and floating zone methods (3). Polycrystalline Si and nanophase Si crystallites are produced by well-known techniques such as gas-phase pyrolysis, photolysis, and discharge cracking of silanes and polysilanes (4, 5).

To date, very little attention has been paid to the production of crystalline Si (or any other group IVA element) by wet-chemical synthesis. Such a synthesis, although unlikely to produce wafer quality Si, could have many advantages. Namely, with this technique it should be possible to control both crystal size and surface functionality, enabling production of well-characterized crystals in the size range below or near the characteristic electronic wavelengths of Si. Such control has been exhibited in a number of syntheses developed over the past few years for the production of the II-VIA (6, 7) and III-VA (8) families of

semiconductor crystals.

I report here a liquid-solution-based technique for the production of micrometer and submicrometer-sized Si single crystals. The synthesis is based on the reduction of $SiCl_4$ and $RSiCl_3$ ($R = H, \text{ octyl}$) in a nonpolar organic solvent (pentane or hexane). The reaction is:



and the function of the R group is discussed later in the text.

This synthesis was carried out in a high-temperature, high-pressure, 300-ml bomb (Parr Instruments) manufactured from the alloy Inconel and equipped with a magnetically coupled stir drive. The bomb was adapted with a syringe inlet port for introduction of reagents and a vacuum port for attachment to a diffusion-pumped vacuum line. Before loading, the bomb was connected to the vacuum line and evacuated to 1×10^{-4} torr for several hours. Hexane (or pentane) was dried over a mixture of Na and benzophenone, and the reactants $SiCl_4$ (99%; Johnson Matthey), $RSiCl_3$ (99%; Johnson Matthey), and 28 to 32% Na dispersion in toluene (Johnson Matthey) were used without further purification. All components (150 ml of hexane, 1 ml of $SiCl_4$, 1 ml of $RSiCl_3$, and 10 ml of Na-toluene dispersion) were transferred into the bomb by either vacuum transfer or clean syringe transfer techniques. The bomb was back-filled with Ar to 1 atm and fitted with a heating mantle. The bomb was

IBM T. J. Watson Research Laboratories, Yorktown Heights, NY 10598.

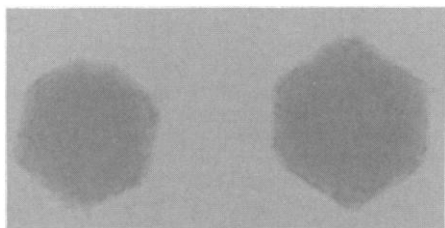


Fig. 1. Transmission electron micrograph taken at 60,000 magnification showing two hexagonal-shaped Si single crystals synthesized by the liquid-solution-phase technique discussed in the text. The crystals are approximately 300 nm in diameter.

heated with rapid stirring to 385°C for 3 to 7 days. Heating caused a pressure increase to >100 atm. After it cooled to room temperature, the bomb was opened to the atmosphere, and the contents were filtered and washed with excess hexane, methanol, ether, and water to remove any remaining Na, NaCl by-product, and hydrocarbon residue. The filtrate was then dried on a vacuum line for further analysis.

Visual inspection with an optical microscope indicated that the crystallites were deep red to yellow, depending on the size and number of crystallites along the axis of view. This is not a quantum effect but is instead the result of a changing opacity of the sample with respect to sample depth. For Si, the optical density increases gradually from the indirect band gap at 1.16 eV to the direct band gap at 3.4 eV (9). A large Si crystal is, apparently, black. However, if it is thinned to the depth of a few micrometers and less, it will change from black to deep red to yellow. In a similar manner, the color of these crystals apparently changes with respect to size. The ultraviolet-visible absorption spectrum of these crystallites, without any size separation, is similar to that of bulk crystalline Si.

Spatially resolved (<1- μm^2 resolution) energy-dispersed x-ray (EDX) analysis of a 2500- μm^2 batch of crystallites supported on an Au grid verified that the dominant element in the material is Si, with only trace amounts of Na and Cl present (<2% each). These measurements, performed on products from a reaction in which the HSiCl_3 reactant was used, indicated that this material was homogeneous over the region scanned. Analysis by EDX also indicated trace amounts of C and O. Similar amounts of C and O, however, were also detected on regions of the Au substrate that did not contain any crystallites, indicating that these elements probably originate from hydrocarbons adsorbed onto the grid and not from the crystallites themselves.

A small amount of material was taken up in hexane and deposited onto an amor-

phous C substrate for transmission electron microscopy (TEM) analysis. Analysis of the $\text{SiCl}_4 + \text{HSiCl}_3$ reaction product revealed a wide size distribution (5 to 3000 nm) of mostly hexagonal-shaped crystals. A TEM micrograph of two such crystals, approximately 300 nm in diameter, is shown in Fig. 1. These crystals are situated such that the [011] zone axis lies very near the plane of the page. Figure 1 shows that these crystals clearly are not aggregates but rather are easily separable. A few of the smaller crystals, however, do appear to be aggregated into groups of two or three. If the particles are ultrasonically dispersed into a 1:1 methanol-acetone solution, they form a poor colloid. They cannot be filtered from the solution but, over a period of a few hours, will slowly settle to the bottom of the container. Further attempts at solvation have not been made.

Selected-area electron diffraction (ED) was performed on several single crystals to verify their structure. Figure 2 shows an ED pattern obtained by rotating the grid so that the [011] zone axis of one of the 300-nm crystals from Fig. 1 is parallel to the plane of view. At the resolution of the apparatus (about 1%), this and other similar patterns exactly match that of a Si single-crystal standard, verifying the presence of diamond-lattice Si single crystals. Some of the material, especially the larger crystallites, is poorly annealed. Although these crystallites are also hexagonally shaped, they give rise to diffraction patterns that are difficult to interpret, and the particles appear to completely amorphize under the influence of the 300-keV electron beam of the microscope. X-ray diffraction of a bulk sample indicates a broad amorphous Si background, with weak diffraction features corresponding to the (111), (311), and (400) planes observed. It is known that, for many materials with crystal size below 1 μm , melting point and crystal size are closely related, with smaller crystals melting at lower temperatures (10). This may also be the case for Si. The synthesis temperature that was used is very low as compared to standard methods for the production of crystalline Si, and thus it may be that only the smallest crystallites are efficiently annealed. Similar reactions have been carried out on $\text{GeCl}_4\text{-RGeCl}_3$ (R = phenyl, Cl), and these reactions go to completion, producing pure nanocrystalline Ge (size <20 nm) (11). The melting point of Ge is approximately 500°C below that of Si, implying that a higher temperature reduction of halosilanes is necessary to drive the Si reaction to completion (12).

The R group in these syntheses serves as a surface-capping agent for the crystals. Therefore, the ratio of the RSiCl_3 to the SiCl_4 reagent should be a measure of the

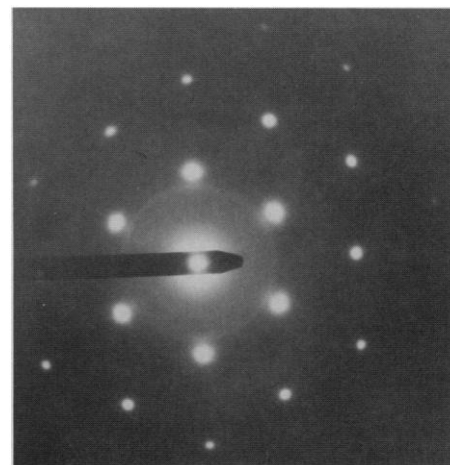


Fig. 2. Selected-area electron diffraction pattern obtained by rotating one of the crystals shown in Fig. 1 such that the [011] crystal zone axis, which is along the plane of the page in Fig. 1, is along the plane of view. This diffraction pattern confirms that these crystals are diamond lattice Si.

surface-to-volume ratio of the final crystallites. The results discussed above for R = H indicate that H is a very poor size controller, yielding clusters from 5 nm to 3 μm . However, for R = octyl, the size is controlled to a diameter of 5.5 ± 2.5 nm. This range was determined by TEM imaging of over 100 particles. No particles smaller than 2 nm or larger than 9 nm were observed. The lack of tails in the size distribution and the fact that the size may be somewhat controlled by introduction of an alkyl group demonstrate the power of a wet chemical synthesis. If organosilanes are pyrolyzed by gas-phase techniques, on the other hand, the product is SiC. The nanocrystals produced by this R = octyl reaction are still faceted, but the yield of crystalline material is apparently below 10%.

Infrared (IR) absorption spectroscopy is a good probe of the surface of these particles. For R = H, IR absorption spectroscopy shows that the crystallites are covered with Si-O and Si-Cl bonds. For R = octyl, this technique shows only weak absorption from hydrocarbon stretching modes, indicating that much of the octyl group is no longer present. Instead, the material appears to be covered with Si-H, Si-O, and Si-Cl bonds. This may be understood in light of the nature of the Si-C bond. This bond is quite polar, with the Si donating electron density onto the C. This will slightly reduce the $\alpha\text{C}-\beta\text{C}$ bond and activate the β -hydrogens. Thus, β -hydride transfer to form a Si-H bond, followed by elimination of 1-octene, will leave Si-H instead of Si-octyl on the surface. The fact that some size control is effected indicates that this reaction occurs at high tempera-

tures, after the chlorosilanes have been reduced and Si-Si bonding networks have formed.

REFERENCES AND NOTES

- For an excellent discussion of modern techniques for the production of crystalline silicon, see: E. Kaldis, Ed., *Crystal Growth of Electronic Materials* (North-Holland, Amsterdam, 1985).
- J. Czochralski, *Z. Phys. Chem. (Frankfurt-am-Mein)* **92**, 219 (1917).
- P. H. Keck and M. J. E. Golay, *Phys. Rev.* **89**, 1297 (1953).
- J. M. Jasinski and F. K. LeGoues, *Chem. Mater.* **3**, 989 (1991).
- H. Takagi *et al.*, *Appl. Phys. Lett.* **56**, 2379 (1990).
- L. E. Brus, *J. Phys. Chem.* **90**, 2555 (1986).
- M. L. Steigerwald *et al.*, *J. Am. Chem. Soc.* **110**, 3046 (1988).
- M. A. Olshavsky, A. N. Goldstein, A. P. Alivisatos, *ibid.* **112**, 9438 (1990).
- M. L. Cohen and T. K. Bergstresser, *Phys. Rev.* **141**, 789 (1966).
- See A. N. Goldstein, C. M. Echer, A. P. Alivisatos, *Science* **256**, 1425 (1992), and references therein.
- J. R. Heath, in preparation.
- We are currently constructing an apparatus in which to carry out such syntheses.
- I acknowledge the assistance of I. J. Fisher and J. Ott in performing the EDX measurements.

31 July 1992; accepted 8 October 1992

Micropaleontological Evidence for Increased Meridional Heat Transport in the North Atlantic Ocean During the Pliocene

Harry J. Dowsett,* Thomas M. Cronin, Richard Z. Poore, Robert S. Thompson, Robin C. Whitley, Adrian M. Wood

The Middle Pliocene (~3 million years ago) has been identified as the last time the Earth was significantly warmer than it was during the Last Interglacial and Holocene. A quantitative micropaleontological paleotemperature transect from equator to high latitudes in the North Atlantic indicates that Middle Pliocene warmth involved increased meridional oceanic heat transport.

Concern about the effects of anthropogenically increased atmospheric concentrations of greenhouse gases has led to increased efforts to understand climates that were warmer than present conditions, such as those of the Late Cretaceous (1), Eocene (2, 3), Middle Pliocene (4), and Last Interglacial (5) (O isotope substage 5e). If a period of warm global climate can be accurately reconstructed from proxy paleoclimate data, then simulation experiments can be used to refine general circulation models and identify mechanisms responsible for the warming (6).

The Pliocene is an ideal interval to test such an approach. First, there is abundant evidence for global warmth. For example, the range of shallow marine and open-ocean faunas as well as terrestrial flora was displaced northward in the North Atlantic and surrounding regions (7-9). Geomorphological and stratigraphical evidence from the eastern United States (10, 11) indicates that sea level was at least 20 m higher than it is today. This height is also

supported by deep-sea isotopic data (12, 13). Such a rise in sea level would require melting of part of the Antarctic ice cap. This potential for melting is confirmed by the occurrence of Pliocene marine diatoms in clasts within the Sirius Formation (Antarctica), which indicates marine conditions in the interior of East Antarctica (14, 15). Sea-surface temperatures of the North Atlantic 3 million years ago (Ma) in some regions are estimated to be more than 8°C higher than those of today (8, 16). In this report we use data from planktic foraminifers, ostracods, pollen, and plant macrofossils to characterize the Pliocene climate and evaluate the gradient of surface temperature in the North Atlantic region.

Many Pliocene marine, and increasing numbers of nonmarine, sites have reliable paleomagnetic and isotopic age control. Estimates of Pliocene environmental conditions are more reliable than those of pre-Pliocene periods because most Pliocene marine and nonmarine species are extant. Thus, Pliocene reconstructions generally have greater environmental and temporal resolution than paleoclimatic reconstructions of earlier times.

The boundary conditions we used for the Middle Pliocene reconstruction are like those of the present with a few notable exceptions. Although some workers have suggested that uplift of the Tibetan Plateau

during the last 3 million years affected climate (17), recent work suggests that the Plateau reached its present elevation at 8 Ma (18) and, therefore, may not have been a primary factor in Pliocene climate change. The Central American Isthmus probably became a barrier to deep circulation during the latest Miocene or earliest Pliocene and a barrier to surface circulation near 3 Ma (19). The Bering Straits, which provide a shallow connection between the Pacific and Arctic oceans (20), opened at 3 Ma or earlier.

From analysis of planktic foraminifers and ostracods we produced a synoptic map of surface temperature for the North Atlantic ocean centered around 3 Ma (Fig. 1). We used factor-analytic transfer functions and dissimilarity coefficient matching techniques for planktic foraminifers (21, 22) and ostracods (7, 23) to estimate conditions of the sea surface and shallow sea bottom from Pliocene samples.

Our results, based on different quantitative methods (species-level factor analysis and dissimilarity coefficient mapping on the

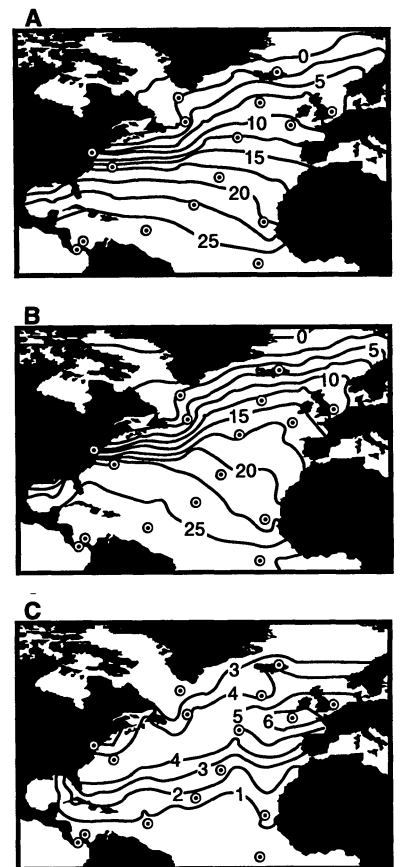


Fig. 1. Maps of (A) modern winter sea-surface temperatures, (B) Pliocene winter sea-surface temperatures, and (C) Pliocene winter sea-surface temperature anomalies (Pliocene minus modern), showing regional distribution of Middle Pliocene warming (in degrees Celsius). Circles show location of deep-sea cores and ocean margin sections used to constrain contours. See (8) for methodology.

H. J. Dowsett, T. M. Cronin, R. Z. Poore, U.S. Geological Survey, Reston, VA 22092.
R. S. Thompson, U.S. Geological Survey, Denver Federal Center, Denver, CO 80225.
R. C. Whitley and A. M. Wood, University College of Wales, Aberystwyth, Wales SY23 3DB, United Kingdom.

*To whom correspondence should be addressed.